**Inhibition by phenolic antioxidants of the degradation of aromatic amines and sulfadiazine by the carbonate radical ($CO_3^{\bullet-}$)**

# Inhibition by phenolic antioxidants of the degradation of aromatic amines and sulfadiazine by the carbonate radical ($CO_3^{\bullet-}$)

**Luca Carena,[a] Davide Vione,[a,*] Marco Minella,[a] Silvio Canonica[b,*] and Ursula Schönenberger[b]**

[a] Università di Torino, Dipartimento di Chimica, Via Pietro Giuria 5, 10125 Torino, Italy.

[b] Eawag, Swiss Federal Institute of Aquatic Science and Technology, Überlandstrasse 133, CH-8600 Dübendorf, Switzerland

[*] Corresponding Authors:

DV: Telephone: +39-011-670-5296. Fax +39-011-670-5242. E-mail: davide.vione@unito.it.

SC: Telephone: +41-58-765-5453. Fax +41-58-765-5028. E-mail: silvio.canonica@eawag.ch.

## *Abstract*

The carbonate radical $CO_3^{\bullet-}$ and the excited triplet states of chromophoric dissolved organic matter play an important role in the photodegradation of some easily oxidized pollutants in surface waters, such as the aromatic amines. Anilines and sulfadiazine are known to undergo back-reduction processes when their degradation is mediated by the excited triplet states of photosensitizers (triplet sensitization). Back-reduction, which inhibits photodegradation, means that phenols or the antioxidant (mostly phenolic) moieties occurring in the natural dissolved organic matter of surface waters reduce, back to the parent compounds, the radical

species derived from the mono-electronic oxidation of anilines and sulfadiazine. Here we show that a similar process takes place as well in the case of substrate oxidation by $CO_3^{\bullet-}$. The carbonate radical was here produced upon oxidation of $HCO_3^-/CO_3^{2-}$ by either $HO^\bullet$, generated by nitrate photolysis, or $SO_4^{\bullet-}$, obtained by photolysis of persulfate. Back-reduction was observed in both cases in the presence of phenols, but at different extents as far as the details of reaction kinetics are concerned, and the occurrence of additional reductants might affect the efficacy by which phenols carry out the reduction process. In particular, when the carbonate radicals were produced by $NO_3^-$ photolysis in the presence of $HCO_3^-/CO_3^{2-}$, the numerical values of $[PhOH]_{1/2}$ (the phenol concentration that halves the photodegradation rate of the substrate) were 2.19 ± 0.23 μM for aniline, 1.15 ± 0.25 μM for 3-chloroaniline, 1.18 ± 0.26 μM for 4-chloroaniline, and 1.18 ± 0.22 μM for 3,4-dichloroaniline. In contrast, when $CO_3^{\bullet-}$ was produced by photolysis of persulfate in the presence of $HCO_3^-/CO_3^{2-}$, the corresponding values were 0.28 ± 0.02 μM for aniline and 0.79 ± 0.10 μM for sulfadiazine. Back-reduction has the potential to significantly inhibit photodegradation by $CO_3^{\bullet-}$ and excited triplet states in natural waters, and to comparatively increase the importance of $HO^\bullet$-mediated degradation that is not affected by the same phenomenon.

**Keywords:** Back-reduction; aniline; phenol; excited triplet states; photochemistry.

# 1. Introduction

Photochemical reactions are important processes for the degradation of organic contaminants, especially biorecalcitrant compounds, in sunlit surface waters. Photoinduced processes consist of the direct photolysis, in which the contaminant absorbs sunlight and gets consequently transformed, and of indirect phototransformation. In the latter, absorption of sunlight by photosensitizers (such as the chromophoric dissolved organic matter – CDOM –, nitrate and nitrite) yields reactive transient species, either directly or upon interaction with the water matrix (e.g., with the inorganic carbon species $HCO_3^-$ and $CO_3^{2-}$). These photochemically produced reactive intermediates (PPRIs) can react with the contaminants. The main PPRIs are the hydroxyl radical ($HO^\bullet$), the triplet states of CDOM ($^3$CDOM*), the singlet oxygen ($^1O_2$) and the carbonate radical ($CO_3^{\bullet-}$) (Boreen et al., 2003; Remucal, 2014; Vialaton and Richard, 2002; Yan and Song, 2014).

The dissolved organic matter (DOM) and its chromophoric fraction (CDOM) play major roles in the photochemistry of natural surface waters. CDOM is a direct or indirect source of all the PPRIs, but it is also able to inhibit the direct photolysis processes by competing with the contaminants for sunlight irradiance. Furthermore, the DOM is a key scavenger of both $HO^\bullet$ and $CO_3^{\bullet-}$ (Vione et al., 2014; Yan et al., 2019). Therefore, the natural organic matter that occurs in surface waters is able to both inhibit and enhance the phototransformation reactions.

In addition to PPRIs scavenging, DOM can inhibit phototransformation through its antioxidant moieties (AOs, mostly phenolic). Indeed, it has been shown that the reactions between $^3$CDOM* and some contaminants (especially aromatic amines) yield partially oxidized intermediates, which can be back-reduced to the parent contaminants by DOM-AOs (Canonica and Laubscher, 2008; Wenk and Canonica, 2012).

68 This back-reduction process does not only affect reactions induced by $^3$CDOM*, but has
69 recently been shown to occur for the reaction of the sulfate radical ($SO_4^{\bullet-}$) with several
70 anilines and sulfonamide antibiotics (Canonica and Schönenberger, 2019) as well as for the
71 reaction of $CO_3^{\bullet-}$ with the cyanotoxin cylindrospermopsin (Hao et al., 2020). Since $CO_3^{\bullet-}$ is a
72 typical one-electron oxidant (Neta et al., 1988) that reacts efficiently with a variety of
73 aromatic amine compounds (Canonica et al., 2005; Huang and Mabury, 2000a, 2000b), it is
74 expected that such compounds are on the one hand significantly oxidized by $CO_3^{\bullet-}$ in the
75 aquatic environment, and experience on the other hand back-reduction by DOM-AOs.
76 Interestingly, occurrence of back-reduction has not been observed in the case of $HO^{\bullet}$, which
77 undergoes addition to aromatic rings more easily than one-electron oxidation or H-atom
78 abstraction (Wenk et al., 2011).
79 The present study has the goal of detecting and quantifying back-reduction by two phenols,
80 used as DOM-AOs surrogates, in the reactions of $CO_3^{\bullet-}$ with several anilines and the
81 sulfonamide antibiotic sulfadiazine. The oxidation of $HCO_3^-/CO_3^{2-}$ to $CO_3^{\bullet-}$ by strongly
82 oxidizing radicals was carried out through two alternative methods (Huang and Mabury,
83 2000a; Neta et al., 1988). The first method is the photolysis of nitrate to yield $HO^{\bullet}$ (Mack and
84 Bolton, 1999), and the second is the photolysis of persulfate ($S_2O_8^{2-}$) to form $SO_4^{\bullet-}$ (Criquet
85 and Leitner, 2009). In addition, the effect of phenol on the transformation of two anilines
86 photosensitized by a model aromatic ketone as a CDOM surrogate was also carried out, with
87 the purpose of comparing the extent of back-reduction among different oxidation reactions.
88

## 2. Materials and Methods

The list of used chemicals is reported in **Text S1** of the Supplementary Material, hereinafter SM. The main issue with the production of $CO_3^{\bullet-}$ is that this radical is generated by oxidation of $HCO_3^-/CO_3^{2-}$. Therefore, the production of $CO_3^{\bullet-}$ requires a stronger oxidant than $CO_3^{\bullet-}$ itself which may, however, be able to compete with $CO_3^{\bullet-}$ for the degradation processes. Great care is thus to be taken to define the operational conditions, so that the chosen oxidant species is almost exclusively involved in the oxidation of inorganic carbon, while the generated $CO_3^{\bullet-}$ reacts preferentially with the target substrates. In this work, two methods were used and compared for the generation of $CO_3^{\bullet-}$: *(i)* oxidation by $HO^{\bullet}$, produced by nitrate photolysis, and *(ii)* oxidation by $SO_4^{\bullet-}$, produced by photolysis of persulfate ($S_2O_8^{2-}$).

### 2.1. Formation of the carbonate radical ($CO_3^{\bullet-}$) by nitrate photolysis

The $CO_3^{\bullet-}$ radicals were produced by irradiation of a mixture of $NaNO_3$ + $NaHCO_3$ (pH 8.3), containing the aniline substrate (target compound TC) to be degraded as well as phenol (PhOH). In particular, TC = aniline (Ani), 3-chloroaniline (3CA), 4-chloroaniline (4CA), and 3,4-dichloroaniline (3,4DCA). Under UVB light nitrate photolyzes and gives $HO^{\bullet}$, which then oxidizes $HCO_3^-/CO_3^{2-}$ to form $CO_3^{\bullet-}$ and $H_2O/HO^-$ (second-order rate constants for the corresponding reactions are defined in parenthesis) (Buxton et al., 1988).

$$NO_3^- + h\nu + H^+ \rightarrow {}^{\bullet}NO_2 + HO^{\bullet} \quad (1)$$

$$HCO_3^- + HO^{\bullet} \rightarrow CO_3^{\bullet-} + H_2O \qquad (k_{HO^{\bullet},HCO_3^-} = 8.5 \times 10^6\ M^{-1}\ s^{-1}) \quad (2)$$

$$CO_3^{2-} + HO^{\bullet} \rightarrow CO_3^{\bullet-} + HO^- \qquad (k_{HO^{\bullet},CO_3^{2-}} = 3.9 \times 10^8\ M^{-1}\ s^{-1}) \quad (3)$$

Photogenerated $^{\bullet}NO_2$ might interfere by reacting with some radical intermediates, but the use of $H_2O_2$ as alternative $HO^{\bullet}$ source was ruled out because $H_2O_2$ also reacts with $HO^{\bullet}$ producing the reductant $O_2^{\bullet-}$, which in turn has high potential to interfere with back-reduction processes (Canonica and Schönenberger, 2019).

In the system containing nitrate and bicarbonate under irradiation, both $HO^{\bullet}$ and $CO_3^{\bullet-}$ could potentially react with TC and PhOH, causing their degradation. Because our aim was to assess the importance of back-reduction in the degradation of TC by $CO_3^{\bullet-}$, the reactions involving $HO^{\bullet}$ + TC, $HO^{\bullet}$ + PhOH and $CO_3^{\bullet-}$ + PhOH had to be minimized (see **Scheme 1**). This goal can be achieved if photogenerated $HO^{\bullet}$ is almost exclusively involved in the oxidation of $HCO_3^-/CO_3^{2-}$ to produce $CO_3^{\bullet-}$.

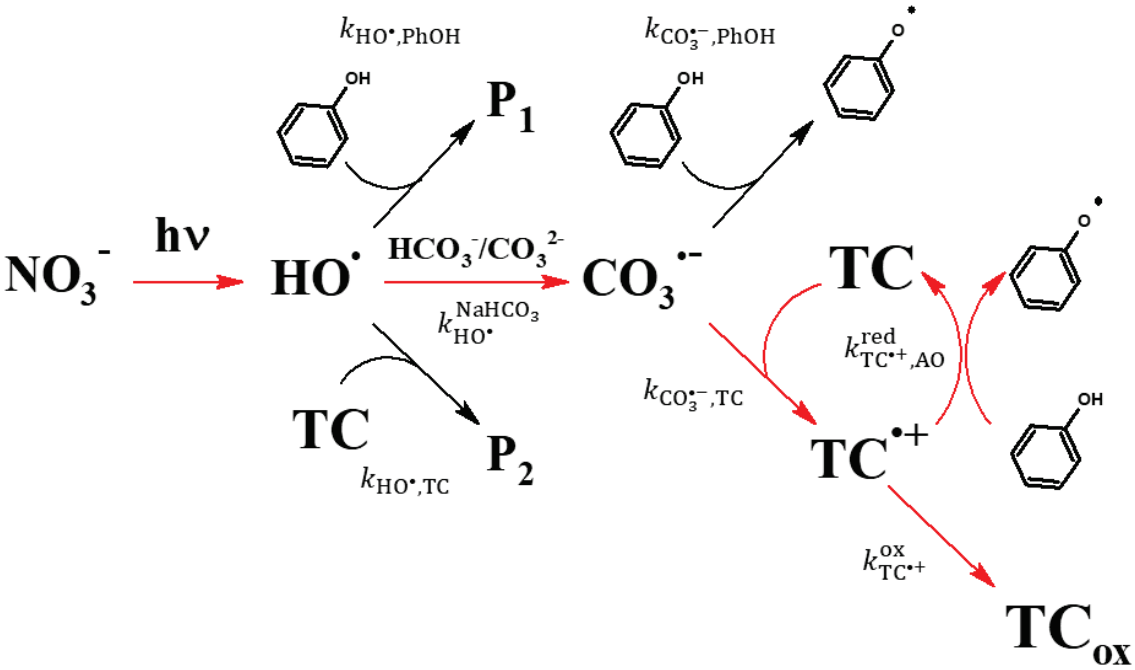


**Scheme 1**. Simplified scheme showing the main reactions taking place in our irradiated solutions, for the assessment of the back-reduction process during TC (anilines) degradation by $CO_3^{\bullet-}$. It is important to choose conditions so that the system follows the reaction pathway highlighted with red arrows.

In other words, the fraction of $HO^{\bullet}$ that reacts with $HCO_3^-/CO_3^{2-}$ ($\chi_{HO^{\bullet}}^{NaHCO_3}$) should be > 95% (**Eq. 4**). Note that $\chi_{HO^{\bullet}}^{NaHCO_3}$ takes into account the $HO^{\bullet}$ reaction with both bicarbonate and carbonate. At the same time, the majority of $CO_3^{\bullet-}$ produced by $HO^{\bullet}$ should react with TC ($\chi_{CO_3^{\bullet-}}^{TC}$ > 95%, **Eq. 5**; see also **Text S2** in the SM).

$$\chi_{HO^{\bullet}}^{NaHCO_3} = \frac{k_{HO^{\bullet}}^{NaHCO_3} \times c_{NaHCO_3}}{k_{HO^{\bullet},TC} \times [TC] + k_{HO^{\bullet},PhOH} \times [PhOH] + k_{HO^{\bullet}}^{NaHCO_3} \times c_{NaHCO_3}} > 0.95 \quad (4)$$

$$\chi_{CO_3^{\bullet-}}^{TC} = \frac{k_{CO_3^{\bullet-},TC} \times [TC]}{k_{CO_3^{\bullet-},TC} \times [TC] + k_{CO_3^{\bullet-},PhOH} \times [PhOH]} > 0.95 \quad (5)$$

In **Eqs. 4,5**, $k_{i,j}$ is the second-order rate constant of the reaction between the radical *i* ($HO^{\bullet}$ or $CO_3^{\bullet-}$) and the species *j* ($HCO_3^-/CO_3^{2-}$, TC or PhOH). Moreover, it is $k_{HO^{\bullet}}^{NaHCO_3} = (k_{HO^{\bullet},HCO_3^-} \times \alpha_{HCO_3^-} + k_{HO^{\bullet},CO_3^{2-}} \times \alpha_{CO_3^{2-}})$, where $\alpha_{HCO_3^-}$ and $\alpha_{CO_3^{2-}}$ are the molar fractions of $HCO_3^-$ and $CO_3^{2-}$ at pH 8.3, computed taking into account the $pK_a$ values of carbonic acid ($pK_{a1}$ = 6.3 and $pK_{a2}$ = 10.3; e.g., Millero et al., 2002). Finally, [*TC*], [*PhOH*] and $c_{NaHCO_3}$ are the respective molar concentrations of TC (fixed at 5 μM; Vione et al., 2018; Wenk and Canonica, 2012), PhOH and $NaHCO_3$ (*vide infra*) added to the solution.

Being the values of $k_{i,j}$ known (see **Table S1** in the SM) (Neta et al., 1988), **Eqs. 4,5** can be solved for the variables [*PhOH*] and $c_{NaHCO_3}$. As a result, one gets the minimum value of $c_{NaHCO_3}$ (0.22-0.38 M, depending on substrate and conditions) and the maximum value of [*PhOH*] (5-8 μM) that should be used to allow for: *(i)* the reactions of $HO^{\bullet}$ with $HCO_3^-/CO_3^{2-}$ to prevail over the reactions of $HO^{\bullet}$ with TC and PhOH, and *(ii)* the reaction $CO_3^{\bullet-}$ + TC to prevail over $CO_3^{\bullet-}$ + PhOH (**Scheme 1**). The complete chemical composition of the irradiated solutions is listed in **Table S1** (SM).

148 To carry out the above experiments, synthetic aqueous solutions (5 mL) were magnetically
149 stirred and irradiated in cylindrical Pyrex glass cells, under a Philips narrow band TL 20W/01
150 lamp. The lamp mainly emits in the UVB wavelength range, with emission maximum at 313
151 nm. The spectral photon flux density ($p^0(\lambda)$, **Fig. S1**, SM) was assessed by means of chemical
152 actinometry with 2-nitrobenzaldehyde (Carena et al., 2019; Galbavy et al., 2010; Willett and
153 Hites, 2000).
154 The direct photolysis can be an additional degradation pathway for TC and, although this
155 process does not affect the branching ratios of the reactions involving $HO^\bullet$ and $CO_3^{\bullet-}$, it is still
156 an experimental bias. Chloro-substituted anilines are known to undergo direct photolysis in
157 the UVB range (**Fig. S2**, SM) (Carena et al., 2018). To minimize their direct photolysis rate,
158 we used a higher $NaNO_3$ concentration (25 mM), exploiting the inner-filter effect of $NaNO_3$,
159 and a lower lamp irradiance (2.9 ± 0.3 W $m^{-2}$). In contrast, aniline did not show direct
160 photolysis, which allowed for the use of lower nitrate (10 mM) and slightly higher lamp
161 irradiance (4.2 ± 0.2 W $m^{-2}$).
162
163 *2.1.1. Modeling TC degradation rate*
164 The degradation rate ($R_{TC}$) of the organic substrate TC (Ani, 3CA, 4CA or 3,4DCA) upon
165 UVB irradiation of a solution containing $NaNO_3$ + $NaHCO_3$ + TC + PhOH is
166 $R_{TC} = R_{CO_3^{\bullet-},TC} + R_{HO^\bullet,TC} + R_{d.p.}$, where $R_{CO_3^{\bullet-},TC}$, $R_{HO^\bullet,TC}$ and $R_{d.p.}$ are the rates of TC
167 degradation by $CO_3^{\bullet-}$, $HO^\bullet$ and the direct photolysis, respectively. Based on the reactions
168 reported in **Scheme 1**, $R_{CO_3^{\bullet-},TC}$ and $R_{HO^\bullet,TC}$ can be expressed as follows:

169 $$R_{CO_3^{\bullet-},TC} = k_{CO_3^{\bullet-},TC} \times [CO_3^{\bullet-}] \times [TC] - k^{red}_{TC^{\bullet+},AO} \times [TC^{\bullet+}] \times [PhOH] \quad (6)$$

170 $$R_{HO^\bullet,TC} = k_{HO^\bullet,TC} \times [HO^\bullet] \times [TC] \quad (7)$$

171 Under the irradiation conditions used in this work, the steady-state approximation can be
172 applied to $HO^{\bullet}$, $CO_3^{\bullet-}$ and $TC^{\bullet+}$. Their steady-state concentrations read as follows:

173 $$[HO^{\bullet}] = \frac{R_{f,HO^{\bullet}}}{k_{HO^{\bullet},TC} \times [TC] + k_{HO^{\bullet},PhOH} \times [PhOH] + k_{HO^{\bullet}}^{NaHCO_3} \times c_{NaHCO_3}} \quad (8)$$

174 $$[CO_3^{\bullet-}] = \frac{k_{HO^{\bullet}}^{NaHCO_3} \times c_{NaHCO_3} \times [HO^{\bullet}]}{k_{CO_3^{\bullet-},TC} \times [TC] + k_{CO_3^{\bullet-},PhOH} \times [PhOH]} \quad (9)$$

175 $$[TC^{\bullet+}] = \frac{k_{CO_3^{\bullet-},TC} \times [CO_3^{\bullet-}] \times [TC]}{k_{TC^{\bullet+},AO}^{red} \times [PhOH] + k_{TC^{\bullet+}}^{ox}} \quad (10)$$

176 By introducing these steady-state concentration values in **Eqs. 6,7** and by considering the
177 definitions of $\chi_{HO^{\bullet}}^{NaHCO_3}$, $\chi_{CO_3^{\bullet-}}^{TC}$ (**Eqs. 4,5**) and $\chi_{HO^{\bullet}}^{TC}$ (see **Text S2**, SM), one gets:

178 $$R_{CO_3^{\bullet-},TC} = R_{f,HO^{\bullet}} \times \chi_{HO^{\bullet}}^{NaHCO_3} \times \chi_{CO_3^{\bullet-}}^{TC} \times \left( \frac{k_{TC^{\bullet+}}^{ox}}{k_{TC^{\bullet+},AO}^{red} \times [PhOH] + k_{TC^{\bullet+}}^{ox}} \right) \quad (11)$$

179 $$R_{HO^{\bullet},TC} = R_{f,HO^{\bullet}} \times \chi_{HO^{\bullet}}^{TC} \quad (12)$$

180 where $R_{f,HO^{\bullet}}$ is the photoproduction rate of $HO^{\bullet}$ upon nitrate photolysis (note that $HO^{\bullet}$ is
181 mostly involved in the generation of $CO_3^{\bullet-}$). It is $R_{f,HO^{\bullet}} \times \chi_{HO^{\bullet}}^{NaHCO_3} \times \chi_{CO_3^{\bullet-}}^{TC} = R_{CO_3^{\bullet-},TC}^{0}$, which is
182 the value of $R_{CO_3^{\bullet-},TC}$ in the absence of phenol ($[PhOH] = 0$). When $[PhOH] = [PhOH]_{1/2}$, one
183 has $R_{CO_3^{\bullet-},TC} = 0.5 \times R_{CO_3^{\bullet-},TC}^{0}$ and $k_{TC^{\bullet+}}^{ox} \times (k_{TC^{\bullet+},AO}^{red} \times [PhOH]_{1/2} + k_{TC^{\bullet+}}^{ox})^{-1} = 0.5$. As a
184 consequence, it is $[PhOH]_{1/2} = k_{TC^{\bullet+}}^{ox} \times (k_{TC^{\bullet+},AO}^{red})^{-1}$ and **Eq. 11** is rearranged as follows:

185 $$R_{CO_3^{\bullet-},TC} = R_{f,HO^{\bullet}} \times \chi_{HO^{\bullet}}^{NaHCO_3} \times \chi_{CO_3^{\bullet-}}^{TC} \times \left( \frac{1}{1 + \frac{[PhOH]}{[PhOH]_{1/2}}} \right) \quad (13)$$

186 Finally, by substituting **Eqs. 12,13** into the expression for $R_{TC}$, one gets **Eq. 14**:

187 $$R_{TC} = R_{f,HO^\bullet} \times \left\{ \chi_{HO^\bullet}^{NaHCO_3} \times \chi_{CO_3^{\bullet-}}^{TC} \times \frac{1}{1+\frac{[PhOH]}{[PhOH]_{1/2}}} + \chi_{HO^\bullet}^{TC} \right\} + R_{d.p.} \quad (14)$$

188 where $\chi_{HO^\bullet}^{NaHCO_3}$ = 0.965 – 0.985 and $\chi_{HO^\bullet}^{TC}$ = 0.016 – 0.018 are the fractions of $HO^\bullet$ that react
189 with, respectively, bicarbonate/carbonate and the anilines (TC) under our experimental
190 conditions ($c_{NaHCO_3}$ = 0.32 – 0.38 M, pH 8.3, $[TC]_0$ = 5 μM), while $\chi_{CO_3^{\bullet-}}^{TC}$ = 0.97 – 0.99 is the
191 fraction of $CO_3^{\bullet-}$ reacting with TC. Note that the formation rate of $CO_3^{\bullet-}$ is
192 $R_{f,CO_3^{\bullet-}} = R_{f,HO^\bullet} \times \chi_{HO^\bullet}^{NaHCO_3} \approx R_{f,HO^\bullet}$. The quantity $[PhOH]_{½}$ is operationally defined as the phenol
193 concentration that halves the rate of TC degradation by $CO_3^{\bullet-}$, compared to the rate observed
194 in the absence of phenol (when $[PhOH]$ = 0, one has $R_{TC} \cong R_{f,HO^\bullet} + R_{d.p.}$; when $[PhOH]$ =
195 $[PhOH]_{½}$, one has $R_{TC} \cong 0.5\, R_{f,HO^\bullet} + R_{d.p.}$). The lower is $[PhOH]_{½}$, the stronger is the
196 inhibition of TC degradation by PhOH through the back-reduction process.
197
198 **2.2. Formation of $CO_3^{\bullet-}$ by persulfate photolysis**
199 The carbonate radical was also generated by photolysis of the persulfate anion in the presence
200 of an excess of bicarbonate anion, according to **Eqs. 15,16** (Huie and Clifton, 1990).

201 $$S_2O_8^{2-} \xrightarrow{h\nu} 2\ SO_4^{\bullet-} \quad (15)$$

202 $$SO_4^{\bullet-} + HCO_3^- \rightarrow SO_4^{2-} + CO_3^{\bullet-} + H^+ \quad (k_{SO_4^{\bullet-},HCO_3^-} = 2.8 \times 10^6\ M^{-1}\ s^{-1}) \quad (16)$$

203 Side-reactions of the sulfate radical anion ($SO_4^{\bullet-}$) are discussed in the following. The
204 carbonate anion ($CO_3^{2-}$) also reacts with $SO_4^{\bullet-}$ ($k_{SO_4^{\bullet-},CO_3^{2-}}$ = 4.1 × $10^6$ $M^{-1}$ $s^{-1}$; Padmaja et al.,
205 1993), but its contribution to $CO_3^{\bullet-}$ formation is only small (i.e., <1.5%) at pH 8.0, which was
206 used in this study. Furthermore, no drawback of this reaction is expected, since no further

reactive species than $CO_3^{\bullet-}$ are produced. The reactions of $SO_4^{\bullet-}$ with organic compounds used in this study are expected to be fast (second-order rate constants up to ~$5 \times 10^9$ $M^{-1}$ $s^{-1}$; Neta et al., 1988). To reduce the transformation of these compounds due to direct reaction with $SO_4^{\bullet-}$, the concentrations of target compounds and the competitor were chosen to be a factor of $10^5$ smaller compared to $HCO_3^-$. $SO_4^{\bullet-}$ can also react with the substrate used for its production (i.e., $S_2O_8^{2-}$), but this reaction channel is estimated to be ~440 times smaller (Herrmann et al., 1995) compared to $CO_3^{\bullet-}$ production. Owing to the low concentration of $S_2O_8^{2-}$ (1 mM), possible products of this reaction are not expected to be relevant for the transformation of the used organic compounds. At the experimental pH, water is a further reactant to be considered for $SO_4^{\bullet-}$ and leads to the formation of hydroxyl radical ($HO^{\bullet}$) (**Eq. 17**) (Herrmann et al., 1995).

$$SO_4^{\bullet-} + H_2O \rightarrow SO_4^{2-} + HO^{\bullet} \qquad (k_{SO_4^{\bullet-},H_2O} = 1.19 \times 10^1\ M^{-1}\ s^{-1}) \qquad (17)$$

The contribution of $HO^{\bullet}$ production from the reaction of $SO_4^{\bullet-}$ with $HO^-$ at pH 8 ([$HO^-$] = 1 μM) is about an order of magnitude smaller compared to water ([$H_2O$] ~ 55 M) (Canonica and Schönenberger, 2019). At the bicarbonate concentration used in this study (0.10 M), $HO^{\bullet}$ formation rates are estimated to be ~390 times lower compared to $SO_4^{\bullet-}$ formation rates. The formed $HO^{\bullet}$ reacts at pH 8 with both $HCO_3^-$ and $CO_3^{2-}$, leading to the formation of $CO_3^{\bullet-}$ (**Eqs. 2,3**). The reactions of $HO^{\bullet}$ with the used organic compounds are expected to be fast (second-order rate constants up to ~ $1 \times 10^{10}$ $M^{-1}$ $s^{-1}$; Buxton et al., 1988), but their importance for the transformation of these compounds is much lower compared to the aforementioned side-reactions of $SO_4^{\bullet-}$, owing to the much lower formation rate of $HO^{\bullet}$ compared to $SO_4^{\bullet-}$. Therefore, the role of $HO^{\bullet}$ would be negligible in the frame of the used conditions.

230

231 *2.2.1. Competition kinetics experiments*

232 Aqueous solutions containing potassium persulfate ($1.0 \times 10^{-3}$ M), sodium bicarbonate ($1.0 \times$
233 $10^{-1}$ M), sulfuric acid (~$0.8 \times 10^{-3}$ M), a single target compound TC (aniline or sulfadiazine,
234 $1.0 \times 10^{-6}$ M), the phenylurea metoxuron (MET) as a competitor ($1.0 \times 10^{-6}$ M), and a
235 variable concentration of either phenol or 4-methylphenol were prepared in quartz glass tubes
236 (18 mm external diameter, 15 mm internal diameter) using appropriate stock solutions of the
237 various components, with pH of 8.0 ± 0.1. This pH was achieved by 1:5 dilution of a sodium
238 bicarbonate stock solution ($5.0 \times 10^{-1}$ M) that was supplemented with two drops of a
239 concentrated sulfuric acid solution (4.6 M). The tubes were closed with glass stoppers, shaken
240 by hand, placed in a water bath and kept 15 minutes at a temperature of 25.0 °C. They were
241 then submitted to irradiation in a temperature-controlled (25.0 ± 0.2 °C) DEMA (Hans
242 Mangels GmbH, Bornhein-Roisdorf, Germany) model 125 merry-go-round photoreactor,
243 which was equipped with a Heraeus Noblelight model TQ718 medium-pressure mercury lamp
244 operated at an input power of 500 W. The lamp was placed in a cooling jacket consisting of a
245 quartz glass inner wall, a borosilicate glass outer wall and a UVW-55 glass filter (supplied by
246 DEMA) in between. The combination of these glasses resulted in a band-pass filter for the
247 wavelength range of 308–410 nm. This setup was chosen, in analogy to previous studies
248 (Canonica and Schönenberger, 2019), to limit the direct phototransformation of the target
249 compounds and the competitor while allowing for photolysis of persulfate, mainly induced by
250 the 313 nm emission line of the mercury lamp. A more detailed description of the
251 photoreactor and its operation is given elsewhere (Wegelin et al., 1994). Samples (400 μL)
252 were taken just before irradiation and during irradiation at regular time intervals, filled into
253 vials and immediately transferred to the refrigerated autosampler (5.0 °C) of the

chromatographic equipment. All kinetic experiments were performed at least in duplicate. Control irradiation experiments were performed with persulfate-free solutions to check for possible interferences by direct or indirect phototransformation reactions of the target compounds and metoxuron (MET). Within the time range employed for competition kinetics experiments, such transformation rates were typically two orders of magnitude lower than the rates induced by $CO_3^{\bullet-}$ in the absence of phenolic inhibitors, but became more important for the higher concentrations of inhibitor. These side-reactions were considered when fitting the data as explained in the Results and Discussion section.

Apparent second-order rate constants for the reaction of $CO_3^{\bullet-}$ with a target compound (TC) leading to the transformation of TC, $k^{\mathrm{tr,app}}_{CO_3^{\bullet-},TC}$, were determined based on the following competition kinetics expression (see **Text S3**, SM for its derivation):

$$\ln \frac{[TC]_0}{[TC]} = \frac{k^{\mathrm{tr,app}}_{CO_3^{\bullet-},TC}}{k^{\mathrm{tr}}_{CO_3^{\bullet-},MET}} \ln \frac{[MET]_0}{[MET]} \qquad (18)$$

where $k^{\mathrm{tr}}_{CO_3^{\bullet-},MET}$ is the second-order rate constant for the reaction of $CO_3^{\bullet-}$ with the competitor MET, leading to the transformation of MET. The term *apparent* ("app" as a superscript in the rate constant) was used to allow for possible side-reactions in the transformation of TC. From the slope $\alpha$ of the regression line of $\ln \frac{[TC]_0}{[TC]}$ vs. $\ln \frac{[MET]_0}{[MET]}$ and the value of $k^{\mathrm{tr}}_{CO_3^{\bullet-},MET}$ = 8.1 $\times$ $10^7$ $M^{-1}s^{-1}$ (value determined by laser flash photolysis; Canonica et al., 2005), the target compound rate constant was obtained as: $k^{\mathrm{tr,app}}_{CO_3^{\bullet-},TC} = \alpha \times k^{\mathrm{tr}}_{CO_3^{\bullet-},MET}$. In consideration of the absence of inhibitory effect due to antioxidant species during the excited-triplet induced oxidation of phenylureas (Canonica and Laubscher, 2008), we made the assumption that $k^{\mathrm{tr}}_{CO_3^{\bullet-},MET}$ remains unaffected by the presence of model antioxidants, such as the employed phenols, in the studied solutions.

276

277 *2.2.2. Inhibitory effect of antioxidants on the second-order rate constant of the carbonate*
278 *radical-induced oxidation of target compounds determined by competition kinetics.*

279 The previously elaborated one-channel model for the oxidation of TC inhibited by an
280 antioxidant (AO) (Canonica and Laubscher, 2008; Wenk et al., 2011) is applied in this section
281 to the derivation of the dependence of $k^{tr}_{CO_3^{\bullet-},TC}$ (see **Text S3**, SM for the definition of this
282 second-order rate constant) on AO concentration, in an analogous manner as performed in the
283 case of the sulfate radical as an oxidant (Canonica and Schönenberger, 2019). We consider
284 the case in which the transformation of TC is exclusively initiated by direct reaction with
285 $CO_3^{\bullet-}$ (i.e., side-reactions of TC can be neglected). The inhibitory effect of an AO on the
286 oxidation of TC is rationalized in terms of the following reaction equations:

287 $$CO_3^{\bullet-} + TC \rightarrow CO_3^{2-} + TC^{\bullet+} \qquad (k^{et}_{CO_3^{\bullet-},TC}) \qquad (19)$$

288 $$TC^{\bullet+} \rightarrow TC_{ox} \qquad (k^{ox}_{TC^{\bullet+}}) \qquad (20)$$

289 $$TC^{\bullet+} + AO \rightarrow TC + AO_{ox} \qquad (k^{red}_{TC^{\bullet+},AO}) \qquad (21)$$

290 where $TC^{\bullet+}$ is the reactive radical intermediate resulting from one-electron oxidation of TC,
291 $k^{et}_{CO_3^{\bullet-},TC}$ is the second-order rate constant for the electron transfer (et) reaction between TC
292 and $CO_3^{\bullet-}$, $k^{ox}_{TC^{\bullet+}}$ is the first-order rate constant for the transformation of $TC^{\bullet+}$ to a stable
293 oxidation product ($TC_{ox}$), and $k^{red}_{TC^{\bullet+},AO}$ is the second-order rate constant for reaction of $TC^{\bullet+}$
294 with AO, which leads to $TC^{\bullet+}$ reduction back to TC and yields an oxidized antioxidant
295 ($AO_{ox}$). The rate equations for TC and $TC^{\bullet+}$ can be expressed as follows:

296 $$\frac{d[TC]}{dt} = -k^{et}_{CO_3^{\bullet-},TC}[CO_3^{\bullet-}][TC] + k^{red}_{TC^{\bullet+},AO}[TC^{\bullet+}][AO] \qquad (22)$$

297 $$\frac{d[TC^{\bullet+}]}{dt} = k^{et}_{CO_3^{\bullet-},TC}[CO_3^{\bullet-}][TC] - k^{red}_{TC^{\bullet+},AO}[TC^{\bullet+}][AO] - k^{ox}_{TC^{\bullet+}}[TC^{\bullet+}] \quad (23)$$

298 Applying the steady-state assumption for $TC^{\bullet+}$ leads to the following equation:

299 $$[TC^{\bullet+}] = \frac{k^{et}_{CO_3^{\bullet-},TC}[CO_3^{\bullet-}][TC]}{k^{ox}_{TC^{\bullet+}} + k^{red}_{TC^{\bullet+},AO}[AO]} \quad (24)$$

300 Substituting $[TC^{\bullet+}]$ from **Eq. 24** into **Eq. 22** and rearranging yields **Eq. 25**:

301 $$\frac{d[TC]}{dt} = -\frac{k^{et}_{CO_3^{\bullet-},TC}}{1 + (k^{red}_{TC^{\bullet+},AO} / k^{ox}_{TC^{\bullet+}})[AO]}[CO_3^{\bullet-}][TC] \quad (25)$$

302 Comparing **Eqs. S5** (see **Text S3**, SM) and **25** leads to the identity:

303 $$k^{tr}_{CO_3^{\bullet-},TC} = \frac{k^{et}_{CO_3^{\bullet-},TC}}{1 + (k^{red}_{TC^{\bullet+},AO} / k^{ox}_{TC^{\bullet+}})[AO]} \quad (26)$$

304 Since AO is generally also transformed during the kinetic runs, $k^{tr}_{CO_3^{\bullet-},TC}$ from **Eq. 26** is
305 properly speaking not a kinetic constant. However, it can be approximated to a constant if
306 [AO] does not deviate strongly from $[AO]_0$ during irradiation. Note that in the case of [AO] =
307 0, $k^{tr}_{CO_3^{\bullet-},TC} = k^{et}_{CO_3^{\bullet-},TC}$.

308

309 **2.3. Back-reduction processes in triplet-sensitized phototransformation**

310 Additional experiments were carried out to investigate back-reduction by phenol during the
311 degradation of 3,4-dichloroaniline (3,4DCA) and 3-chloroaniline (3CA) with excited triplet
312 states. Back-reduction is known to be operational in the degradation of aniline and 4-
313 chloroaniline by $^3$CDOM* (Canonica and Laubscher, 2008; Wenk and Canonica, 2012). The
314 anionic form of 4-carboxybenzophenone (benzophenone-4-carboxylate, hereafter CBBP) was
315 here used as CDOM proxy. Indeed, CBBP has already been employed to this purpose and to

316 determine representative second-order rate constants for the reactions between organic
317 substrates and $^{3}$CDOM* (Carena et al., 2019; Vione et al., 2018). Solutions containing CBBP
318 were irradiated under a UVA black lamp (Philips TL-D 18 W) with emission maximum at
319 369 nm, which produced a UV irradiance of 42.6 ± 0.7 W $m^{-2}$ on top of the irradiated systems
320 (**Fig. S1**, SM). A detailed description of this irradiation setup is reported in Carena et al.
321 (2019). The initial concentrations of TC and CBBP were 5 and 70 μM, respectively, while
322 PhOH was varied between 0 and 10 μM. The pH of the solutions was ~7 and did not vary
323 significantly during irradiation. Buffers were not used in these experiments to avoid unwanted
324 side-reactions. The direct photolysis of 3,4DCA and 3CA was negligible under UVA
325 irradiation during the experimental time interval (4 h irradiation).
326
327 **2.4. Analytical Methods.**
328 The concentration of target compounds during kinetic runs was followed by high-performance
329 liquid chromatography (HPLC) using an Agilent 1100 system equipped with a quaternary
330 low-pressure mixing gradient pump, a refrigerated autosampler, a temperature-controlled
331 column compartment, a diode array detector and an Agilent 1200 fluorescence detector.
332 Alternatively, an analogous Thermo Fisher Ultimate 3000 HPLC system or a VWR-Hitachi
333 LaChrom Elite chromatograph (**Text S4**, SM) were used. A detailed list of HPLC analysis
334 methods is given in **Table S2**, SM.
335

## 3. Results and Discussion

### 3.1. Comparison of back-reduction in $CO_3^{\bullet-}$-induced (nitrate photolysis system) and triplet-sensitized transformation

The degradation of anilines by $CO_3^{\bullet-}$ (produced upon oxidation of $HCO_3^-/CO_3^{2-}$ by $HO^\bullet$, generated by nitrate photolysis) was inhibited when increasing the concentration of added phenol (PhOH, **Fig. S2**, SM). The experimental conditions were chosen to minimize the scavenging of either $CO_3^{\bullet-}$ or $HO^\bullet$ by phenol, a process that would inhibit aniline degradation in a similar way as back-reduction. By excluding scavenging of $CO_3^{\bullet-}/HO^\bullet$, it is possible to arguably assume that the observed inhibition was due to the reactions (back-reduction) between phenol and the one-electron oxidized intermediates formed upon transformation of the anilines (**Scheme 1**).

Assuming $R_{TC} = R_{CO_3^{\bullet-},TC} + R_{HO^\bullet,TC} + R_{d.p.}$ as per *Section 2.1.1* and taking into account the possible back-reduction process, $R_{TC}$ can be expressed as **Eq. 14** that was written in close analogy to the kinetic equations used in previous works, to describe back-reduction in the triplet-sensitized phototransformation of organic compounds (Vione et al., 2018; Wenk et al., 2011; Wenk and Canonica, 2012).

The rate of TC direct photolysis ($R_{d.p.}$) was assessed by correcting the direct photolysis rate measured in ultrapure water ($R_{d.p.,exp}$; see **Fig. S2**, SM for the experimental data) for the inner-filter effect of nitrate (the direct photolysis of TC is slower in the presence of nitrate, **Eq. 27**; Carena et al., 2018).

$$R_{d.p.} = \frac{\int_\lambda p°(\lambda) \times \frac{\varepsilon_{TC}(\lambda) \times [TC]}{\varepsilon_{NO_3^-}(\lambda) \times [NO_3^-] + \varepsilon_{TC}(\lambda) \times [TC]} \times \left[1 - 10^{-b \times (\varepsilon_{NO_3^-}(\lambda) \times [NO_3^-] + \varepsilon_{TC}(\lambda) \times [TC])}\right] d\lambda}{\int_\lambda p°(\lambda) \times \left[1 - 10^{-\varepsilon_{TC}(\lambda) \times b \times [TC]}\right] d\lambda} \times R_{d.p.,exp} \quad (27)$$

In **Eq. 27**, $p°(\lambda)$ is the UVB lamp photon flux density incident over the solution, $\varepsilon(\lambda)$ is a molar absorption coefficient (of TC or $NO_3^-$), and $b$ is the solution optical path length (0.4 cm). The correction factor was ~ 0.94 ($R_{d.p.} \approx 0.94\ R_{d.p.,exp}$). Note that $R_{d.p.}$ was here considered not to vary with [*PhOH*], because the direct photolysis of chloroanilines should occur *via* loss of chlorine atoms rather than through photoionization of the amino group (Carena et al., 2018). Consequently, back reduction by PhOH should not affect the direct photolysis process.

**Fig. 1** shows the experimental profiles of $R_{TC}$ vs. [*PhOH*] for the studied anilines. A very good fit to the experimental data was obtained with **Eq. 14**, which suggests that the kinetic model proposed for back-reduction matches the experimental findings. The calculated $R_{d.p.}$ values (**Eq. 27**) were 0.49 ± 0.03 nM $s^{-1}$ for 3CA, 3.4 ± 0.5 nM $s^{-1}$ for 4CA, and 0.44 ± 0.02 nM $s^{-1}$ for 3,4DCA. Direct photolysis was negligible in the case of Ani. The values of $R_{f,HO^\bullet}$ (**Eq. 14**) obtained from data fit were 2.1 ± 0.1 nM $s^{-1}$ for Ani, 6.3 ± 0.4 nM $s^{-1}$ for 3CA, 4.3 ± 0.5 nM $s^{-1}$ for 4CA, and 3.9 ± 0.3 nM $s^{-1}$ for 3,4DCA. Data fit also yielded $[PhOH]_{½}$ = 2.19 ± 0.23 µM for Ani, 1.15 ± 0.25 µM for 3CA, 1.18 ± 0.26 µM for 4CA, and 1.18 ± 0.22 µM for 3,4DCA.

Interestingly, **Fig. 2** shows that the values of $[PhOH]_{½}$ obtained for the degradation of the anilines by $CO_3^{\bullet-}$ do not significantly differ from those observed in triplet-sensitized oxidation induced by the triplet states of benzophenone-4-carboxylate ($^3$CBBP*) and 2-acetonaphthone ($^3$2AN*). This finding suggests that $CO_3^{\bullet-}$, $^3$CBBP* and $^3$2AN* produce the same intermediates upon aniline oxidation, which all undergo a similar back-reduction process in the presence of PhOH.

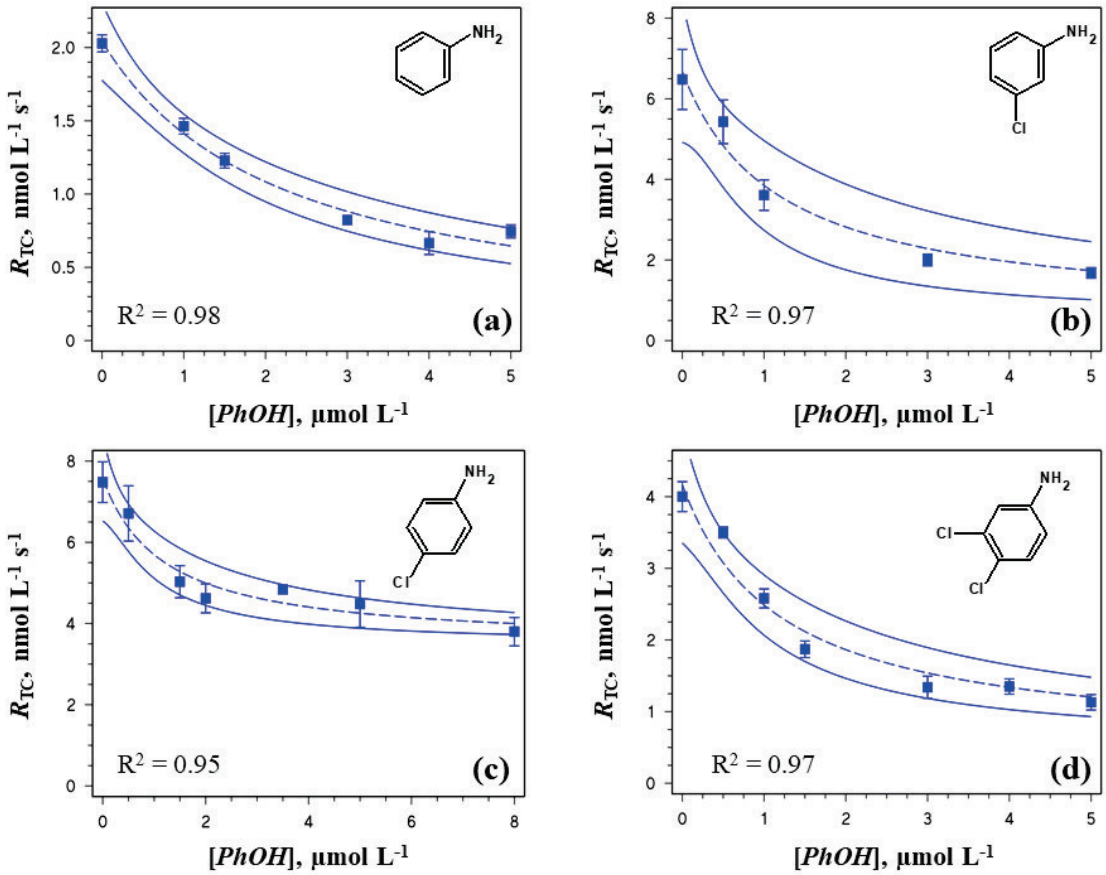


**Figure 1**. Experimental degradation rates of **(a)** Ani, **(b)** 3CA, **(c)** 4CA and **(d)** 3,4DCA (initial concentration 5 µM), as a function of the concentration of added phenol. The dashed curves represent the fit results with **Eq. 14**, while the solid curves are the 95% confidence bands of the fit. The $R^2$ parameter shows the goodness of the fit. The error bounds to the $R_{TC}$ data represent the associated sigma-level uncertainty. The irradiated solutions (pH 8.3) contained $NaNO_3$ + $NaHCO_3$ and were exposed to UVB radiation. See **Table S1**, SM for the detailed experimental conditions.

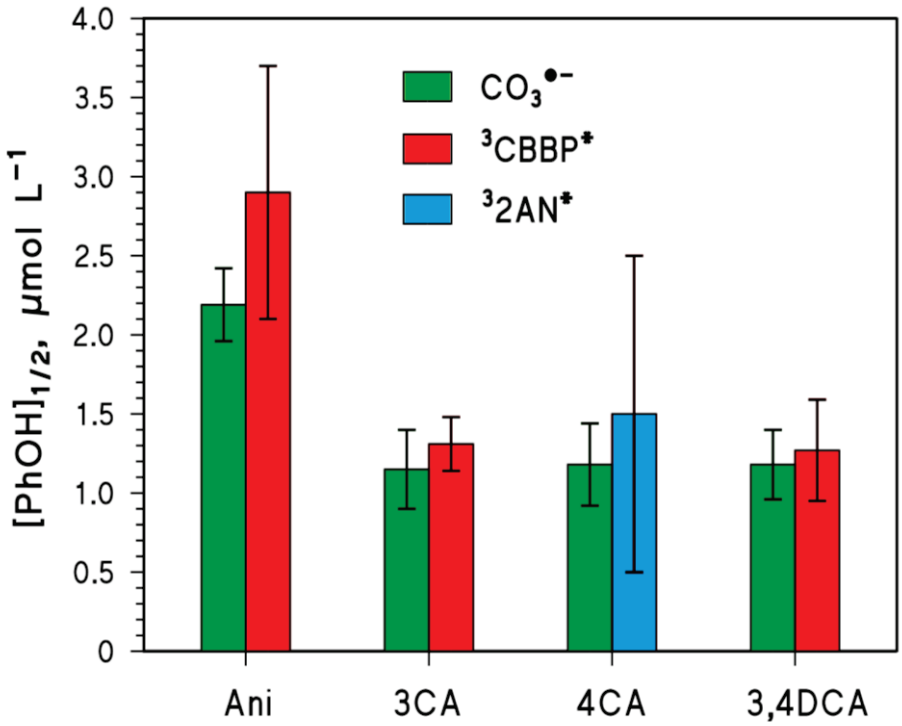


**Figure 2**. Comparison between the $[PhOH]_{1/2}$ values measured for anilines degradation by $CO_3^{\bullet-}$, and those observed for $^3$CBBP*- and $^3$2AN*-induced oxidation. Data concerning the reaction 4CA + $^3$2AN* were taken from Wenk and Canonica (2012), those for Ani + $^3$CBBP* were taken from Canonica and Laubscher (2008), while those for 3CA/3,4DCA + $^3$CBBP* are from this work (**Text S5**, SM). Error bars represent standard errors (in the case of data from this work, they represent the goodness of the fit of the experimental data with **Eq. S10** (SM).

### 3.2. Back-reduction processes upon generation of $CO_3^{\bullet-}$ by $SO_4^{\bullet-}$ as reactive intermediate

Initially, competition kinetics experiments were performed for individual target compounds (TC), i.e., aniline and sulfadiazine, in the absence of phenolic inhibitors. Analogous experiments were also executed for phenol and 4-methylphenol as antioxidant compounds.

These experiments yielded second-order rate constants for the reaction of TC with $CO_3^{\bullet-}$ in the absence of additives, which are termed as $k^{tr}_{CO_3^{\bullet-},TC}$ and provided in **Table 1**. The determined $k^{tr}_{CO_3^{\bullet-},TC}$ values are within a factor of two compared to those known from the literature.

Interestingly, the determined $CO_3^{\bullet-}$ rate constants for phenol and 4-methylphenol are at least 11 and 3 times lower, respectively, compared to the rate constants for aniline and sulfadiazine. This represents an obvious experimental advantage, since these phenols are more resistant to direct $CO_3^{\bullet-}$-induced transformation, and consequently expected to persist and exert their inhibitory effect during the whole course of TC transformation. Examples of kinetics runs showing the transformation of aniline as TC and metoxuron (MET) as competitor in the presence and absence of 0.5 μM phenol as inhibitor are provided in **Figure 3a**, which also shows the transformation kinetics of phenol. All compounds exhibit zero-order kinetics, i.e., a linear decrease in their residual concentration with irradiation time. For the system with aniline and metoxuron without added phenol, this is an indication that aniline, which reacts much faster than metoxuron, is the major species responsible for the scavenging of $CO_3^{\bullet-}$ during the whole kinetic run, and that no reaction products significantly reacting with $CO_3^{\bullet-}$ are formed. Indeed, if $R_{CO_3^{\bullet-}}$ is the formation rate of $CO_3^{\bullet-}$, if $R_{TC} = k^{tr}_{CO_3^{\bullet-},TC}$ [TC] [$CO_3^{\bullet-}$] and if $CO_3^{\bullet-}$ mainly reacts with TC, it is [$CO_3^{\bullet-}$] ≅ $R_{CO_3^{\bullet-}}$ ($k^{tr}_{CO_3^{\bullet-},TC}$ [TC])$^{-1}$ and $R_{TC} \cong R_{CO_3^{\bullet-}}$, which means that $R_{TC}$ is independent of [TC] (zero-order kinetics).

**Table 1.** Second-order rate constants for the reaction of the carbonate radical with target compounds, determined in this study by competition kinetics at pH 8.0±0.1 [a]

| Target compound | $\alpha$ [b] | $k^{tr}_{CO_3^{\bullet-},TC}$ / $10^7$ $M^{-1}$ $s^{-1}$ | | $pK_a$ [c] (literature values) |
|---|---|---|---|---|
| | | this study [d] | literature values [e] | |
| Aniline | 6.12 ± 0.13 | 50 ± 1 | 46 – 67 | 4.60 |
| Sulfadiazine | 6.80 ± 0.10 | 55 ± 1 | 27.8, 28 | 6.5, [f] 6.4 [g] |
| Phenol | 0.435 ± 0.008 | 3.5 ± 0.2 | 0.49 – 2.2 [h] | 9.99 |
| 4-Methylphenol | 1.58 ± 0.03 | 12.8 ± 0.2 | 15 [i] | 10.26 |

[a] Composition of the solutions used for competition kinetics experiments: initial target compound and metoxuron concentrations ($1.0 \times 10^{-6}$ M); potassium persulfate ($1.0 \times 10^{-3}$ M); sodium bicarbonate ($1.0 \times 10^{-1}$ M); sulfuric acid (~$0.8 \times 10^{-3}$ M). [b] Slope $\alpha$ of the competition kinetics plots according to **Eq. 18**, obtained by linear regression, and corresponding to $k^{tr}_{CO_3^{\bullet-},TC} / k^{tr}_{CO_3^{\bullet-},MET}$. The average values from at least two independent experiments are given. The errors represent 95% confidence intervals obtained from linear regression and by applying Gaussian error propagation. [c] $pK_a$ values (from Dean, 1999, except where noted) refer to the following deprotonation equilibria: a) for aniline (An): $AnH^+$/An; b) for sulfadiazine (SD): SD/SD(-H)$^-$ (i.e., second $pK_a$ or $pK_{a2}$); for the phenols (R-PhOH): R-PhOH/R-PhO$^-$. [d] Calculated as $\alpha \times k^{tr}_{CO_3^{\bullet-},MET}$, where the second-order rate constant for the reaction of the carbonate radical with metoxuron was set as $k^{tr}_{CO_3^{\bullet-},MET}$ = $8.1 \times 10^7$ $M^{-1}$ $s^{-1}$. The error in $k^{tr}_{CO_3^{\bullet-},MET}$ ($0.6 \times 10^7$ $M^{-1}$ $s^{-1}$; Canonica et al., 2005) was not considered in the calculation of the errors, which represent 95% confidence intervals. [e] Range of values from Wojnárovits et al., 2020. [f] Boreen et al., 2005. [g] Ricci and Cross, 1993. [h] At pH 7.0 or 8.0. [i] At pH 8.3.

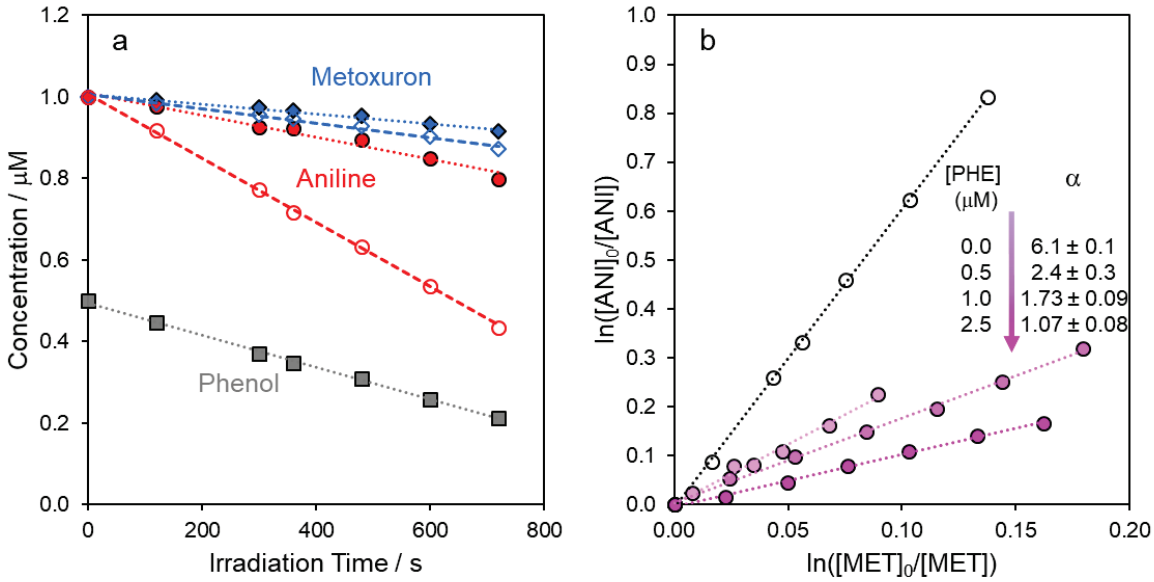


**Figure 3. (a)** Kinetic runs for aniline (red circles) and metoxuron (blue diamonds) in the presence (filled symbols) and absence (open symbols) of 0.5 µM phenol (grey filled squares). The lines represent linear regressions. **(b)** Competition kinetics plots for aniline (1.0 µM initial concentration) as target compound and metoxuron (1.0 µM initial concentration) as competitor, for several different phenol concentrations indicated numerically. The intensity of the filling of the markers increases with increasing phenol concentration. The lines represent linear regressions of the various experimental runs, and their slope $\alpha$ is shown numerically as a function of phenol concentration.

In the absence of phenol, the depletion of both aniline and MET is faster than in its presence, but the reduction in depletion rate is more important for aniline. **Figure 3b** displays competition kinetics examples for the same compounds and different concentrations of added phenol. The slope of the regression lines (defined above as $\alpha$ and given numerically in the graph as a function of the concentration of added phenol) decreases with increasing phenol concentration, indicating a concomitantly decreasing $k^{\mathrm{tr,app}}_{CO_3^{\bullet-},\mathrm{aniline}}$. The trend in $\alpha$ shown in **Figure 3b** clearly demonstrates the inhibitory effect of phenol on the transformation of aniline

induced by $CO_3^{\bullet-}$. Based on **Eq. 26**, we define here the inhibition factor, *IF*, in analogy to previous studies as the ratio between $k^{\mathrm{tr,app}}_{CO_3^{\bullet-},TC}$ and $k^{\mathrm{tr}}_{CO_3^{\bullet-},TC}$, where the latter is the second-order rate constant for the transformation of TC induced by $CO_3^{\bullet-}$ determined without antioxidant addition.

$$IF([AO]) = k^{\mathrm{tr,app}}_{CO_3^{\bullet-},TC} / k^{\mathrm{tr}}_{CO_3^{\bullet-},TC} \quad (28)$$

Substituting the right-hand term of **Eq. 26** into **Eq. 28** yields:

$$IF([AO]) = \frac{1}{1 + (k^{\mathrm{red}}_{TC^{\bullet+},AO} / k^{\mathrm{ox}}_{TC^{\bullet+}}) \times [AO]} \quad (29)$$

With $[AO]_{1/2} = k^{\mathrm{ox}}_{TC^{\bullet+}} / k^{\mathrm{red}}_{TC^{\bullet+},AO}$, **Eq. 29** transforms to:

$$IF([AO]) = \frac{1}{1 + [AO]/[AO]_{1/2}} \quad (30)$$

Series of competition kinetics experiments were performed for the two target compounds, namely aniline and sulfadiazine, using phenol and, alternatively, 4-methylphenol as antioxidants. The results of these experiments are shown in **Figure 4** in terms of inhibition factor as a function of AO concentration. For all four target compound/antioxidant pairs, a decrease in *IF* with increasing [*AO*] is observed. The four *IF* data series were fitted to the following **Eq. 31**, which is a slightly modified form of **Eq. 30** and is used to account for possible side-reactions of the target compounds in analogy to previous studies (Wenk et al., 2011; Wenk and Canonica, 2012).

$$IF([AO]) = \frac{f}{1 + [AO]/[AO]_{1/2}} + (1 - f) \quad (31)$$

Here $f$ is the fraction of TC reacting through the main pathway that is inhibited by antioxidants. For aniline, fits yielded identical $[AO]_{1/2}$ values for phenol (0.28 ± 0.02 μM) and 4-methylphenol (0.28 ± 0.04 μM). For sulfadiazine, fitted $[AO]_{1/2}$ values were 0.79 ± 0.10 μM

for phenol and 0.67 ± 0.06 µM for 4-methylphenol, and therefore higher compared to aniline by a factor of 2.4 and 2.8, respectively. Obtained *f* values were high, namely 0.78 for the pair sulfadiazine/phenol and > 0.92 for all other TC/AO pairs, indicating the minor importance of side-reactions not subject to inhibition by AO.

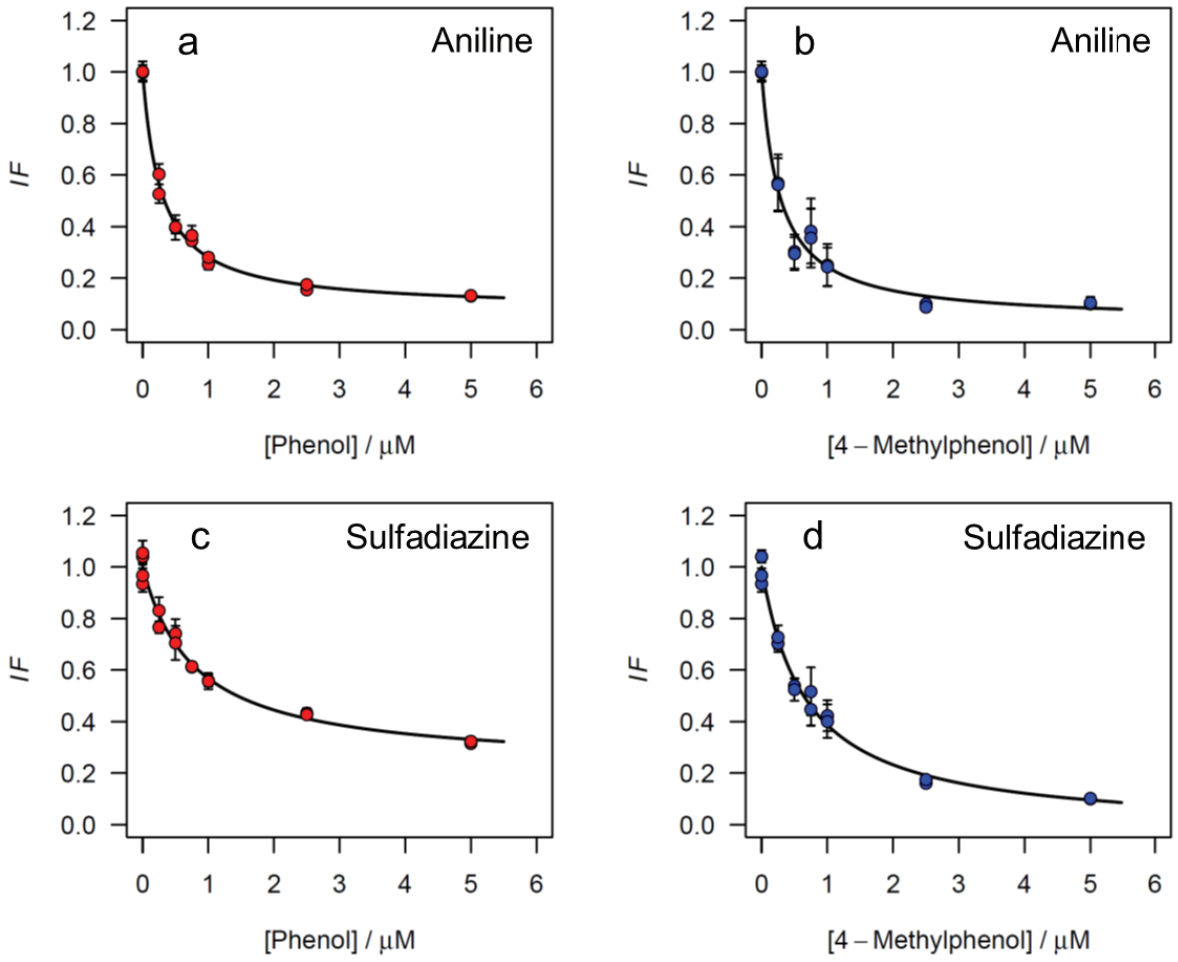


**Figure 4.** Inhibition factors (*IF*) for aniline **(a, b)** and sulfadiazine **(c, d)** determined at pH 8.0 in duplicate at various concentrations of added phenol (left panels) and 4-methylphenol (right panels), respectively, in the range of 0.0 – 5.0 µM. Error bars correspond to 95% confidence intervals obtained from linear regression by applying **Eq. 18** and Gaussian error propagation rules. Black lines are best fitting functions according to **Eq. 31**.

In the case of aniline, it is interesting to observe that the value of $[PhOH]_{½}$ (AO = phenol) is lower by an order of magnitude compared to the value obtained when $CO_3^{\bullet-}$ was produced by nitrate photolysis (see **Section 3.1**). It is also an order of magnitude lower compared to the values determined for triplet-sensitized aniline transformation, conducted using CBBP and 2-AN as photosensitizers (Canonica and Laubscher, 2008; Wenk and Canonica, 2012). All these $[PhOH]_{½}$ values were obtained from experiments carried out at very similar pH values (8.0 – 8.3). Therefore, the slight changes in speciation of the various species involved in the back-reduction process are probably not the cause of the differences in $[PhOH]_{½}$.

Anilines (Ar-$NH_2$) undergo mono-electronic oxidation by $CO_3^{\bullet-}$ (Elango et al., 1984; Huang and Mabury, 2000a; Jonsson et al., 1994; Liu et al., 2018; Wojnárovits et al., 2020) and by the triplet states of 2-acetonapthone ($^3$2AN*) and benzophenone-4-carboxylate ($^3$CBBP*) (Canonica and Laubscher, 2008; Vione et al., 2018; Wenk and Canonica, 2012), forming radical cations (Ar-$NH_2^{\bullet+}$) that easily deprotonate to produce Ar-$NH^{\bullet}$. Previous works have shown that phenolic compounds including phenol (PhOH) can act as antioxidants for the species Ar-$NH^{\bullet}$ (Canonica and Laubscher, 2008; Vione et al., 2018; Wenk and Canonica, 2012). Therefore, the following reactions should take place in the studied systems (where T* represents an excited triplet state, such as that of $^3$2AN*):

$$\text{Ar-NH}_2 + \text{CO}_3^{\bullet-} \rightarrow \text{Ar-NH}_2^{\bullet+} + \text{CO}_3^{2-} \quad (32)$$

$$\text{Ar-NH}_2 + \text{T}^* \rightarrow \text{Ar-NH}_2^{\bullet+} + \text{T}^{\bullet-} \quad (33)$$

$$\text{Ar-NH}_2^{\bullet+} \leftrightarrows \text{Ar-NH}^{\bullet} + \text{H}^+ \quad (34)$$

$$\text{Ar-NH}^{\bullet} \rightarrow \text{oxidized products} \quad (35)$$

$$\text{Ar-NH}^{\bullet} + \text{PhOH} \rightarrow \text{Ar-NH}_2 + \text{PhO}^{\bullet} \quad (36)$$

A possibility to account for differences in the $[PhOH]_{½}$ values observed in different systems is to assume that antioxidant compounds are produced even in the absence of added PhOH,

thereby providing a baseline level of back-reduction (Canonica and Schönenberger, 2019). Such a process would decrease the steady-state [*Ar-NH*$^{\bullet}$] with the consequence that, the higher the baseline reductants, the higher is the concentration of PhOH (quantified as $[PhOH]_{½}$) required to obtain the same *IF* value. Therefore, different systems could show varying levels of baseline back-reduction and provide different values of $[PhOH]_{½}$. A potential photogenerated reductant is superoxide, $O_2^{\bullet-}$, which is for instance produced by reaction between $T^{\bullet-}$ and dissolved oxygen (Canonica and Schönenberger, 2019; Huber et al., 2003). Moreover, the one-electron oxidation of anilines is well known to produce phenolic intermediates (Bossmann et al., 1998) that might act as baseline antioxidants.

As far as back-reduction in sulfadiazine transformation is concerned, the $[PhOH]_{½}$ value found in this study (0.79 ± 0.10 μM) is well matched with $[PhOH]_{½}$ = 0.86 ± 0.10 μM that was obtained for the transformation of sulfadiazine photosensitized by CBBP at pH 8.5 (Vione et al., 2018), but four times lower than a previously determined value (3.2 ± 0.8 μM) for triplet-sensitized transformation at pH 8.0 (Wenk and Canonica, 2012). Therefore, for sulfadiazine the presence of possible baseline antioxidants appears to play a less important role than in the case of aniline.

### 3.3. Environmental significance

To assess the role of back-reduction on the phototransformation of water pollutants, the photochemical fate of aniline was modeled in a lake-water scenario by means of the APEX software (**Figure 5**) (Vione, 2020).

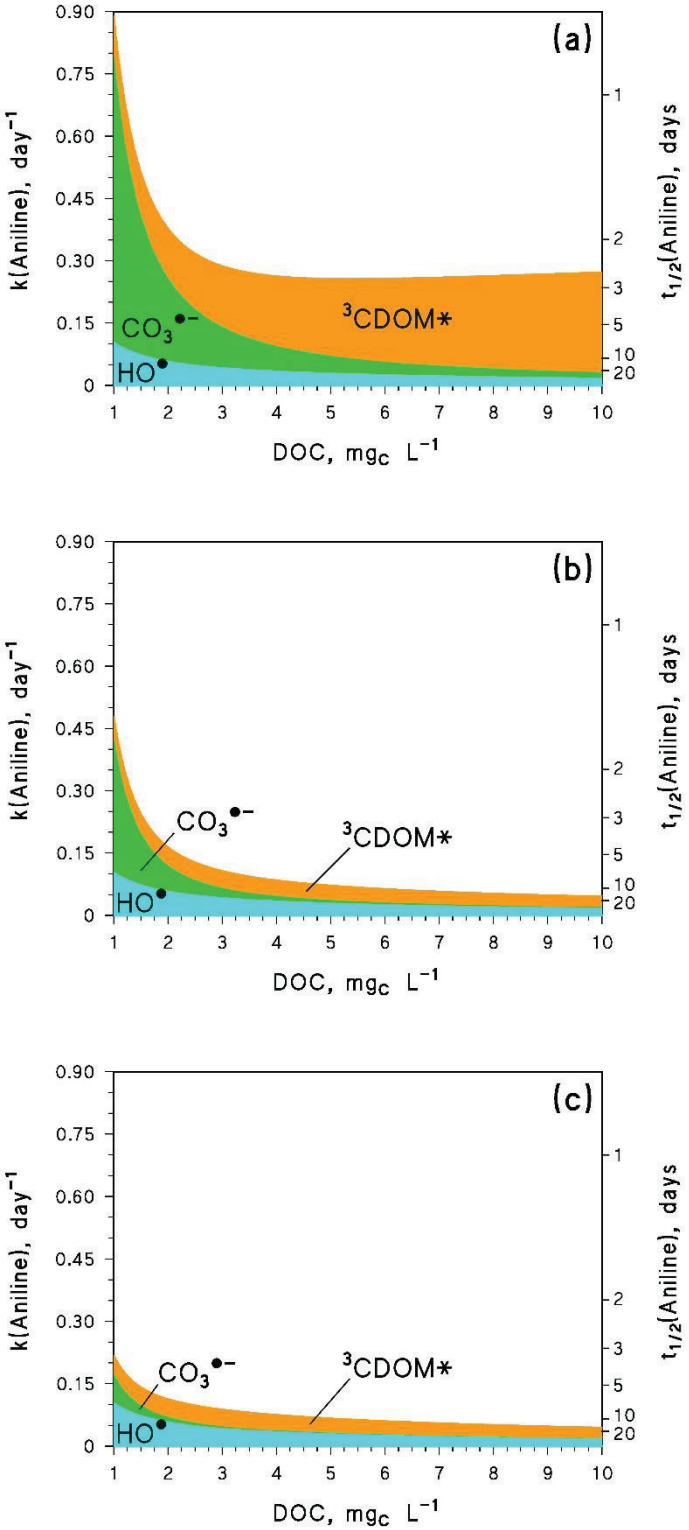


**Figure 5**. Modeled photochemical pseudo-first-order degradation rate constant (left Y-axis) and half-life time (right Y-axis) of aniline in lake water, as a function of the DOC (dissolved organic carbon). **(a)** Scenario 1 (no back reduction); **(b)** Scenario 2 (back reduction for $^3$CDOM*, moderate back reduction for $CO_3^{\bullet-}$); **(c)** Scenario 3 (back reduction for $^3$CDOM*, strong back reduction for $CO_3^{\bullet-}$). Other conditions: 100 µmol L$^{-1}$ $NO_3^-$, 1 µmol L$^{-1}$ $NO_2^-$, 2 mmol L$^{-1}$ alkalinity, pH 8.0, 1 m depth, sunlight irradiance as per mid-July, mid latitude, northern hemisphere.

Aniline was chosen here because two alternative values of $[PhOH]_{½}$ were obtained in this work for this compound, which could be observed under different conditions as far as transformation by $CO_3^{\bullet-}$ is concerned. Aniline does not undergo direct photolysis to a significant extent, but it reacts with $HO^{\bullet}$ (second-order rate constant $k^{tr}_{HO^{\bullet},Ani} = 1.4\times10^{10}$ $M^{-1}$ $s^{-1}$; Buxton et al., 1988), $CO_3^{\bullet-}$ ($k^{tr}_{CO_3^{\bullet-},Ani} = 5\times10^{8}$ $M^{-1}$ $s^{-1}$, this work) and $^3$CDOM* ($k^{tr}_{^3CDOM^*,Ani} = 4\times10^{9}$ $M^{-1}$ $s^{-1}$; estimated from values published by Erickson et al., 2015, for several anilines using methylene blue as model photosensitizer). In the case of natural waters, the natural organic matter is the provider of phenolic antioxidant moieties. The experimental $[PhOH]_{½}$ values can be translated into $DOC_{½}$ equivalents as $DOC_{½}$ ($mg_C$ $L^{-1}$) = 0.4×$[PhOH]_{½}$ (μM), as reported by Vione et al. (2018) (see also Leresche et al., 2016). In the case of aniline + $HO^{\bullet}$, no back-reduction is expected (Wenk et al., 2011). In the case of aniline + $^3$CDOM*, one has $[PhOH]_{½}$ = 2.8 μM ⇒ $DOC_{½}$ = 1.1 $mg_C$ $L^{-1}$ (Wenk and Canonica, 2012). In the case of aniline + $CO_3^{\bullet-}$ (this work), one has either $[PhOH]_{½}$ = 0.28 μM ⇒ $DOC_{½}$ = 0.11 $mg_C$ $L^{-1}$, or $[PhOH]_{½}$ = 2.2 μM ⇒ $DOC_{½}$ = 0.88 $mg_C$ $L^{-1}$.

Here, three different scenarios are considered. In the first (Scenario 1), no back-reduction is supposed to be operational with either $^3$CDOM* or $CO_3^{\bullet-}$. In Scenario 2, we used $DOC_{½}$ = 1.1 $mg_C$ $L^{-1}$ for the $^3$CDOM* process and $DOC_{½}$ = 0.88 $mg_C$ $L^{-1}$ for $CO_3^{\bullet-}$ (moderate back-reduction for $CO_3^{\bullet-}$). In Scenario 3, we used again $DOC_{½}$ = 1.1 $mg_C$ $L^{-1}$ for $^3$CDOM* but $DOC_{½}$ = 0.11 $mg_C$ $L^{-1}$ for $CO_3^{\bullet-}$ (strong back-reduction for $CO_3^{\bullet-}$).

**Figure 5** shows that, in the absence of back-reduction (**5a**), $CO_3^{\bullet-}$ is the main aniline photodegradation process at low DOC while $^3$CDOM* prevails at high DOC (indeed, $CO_3^{\bullet-}$ is very efficiently scavenged by DOM; Yan et al., 2019). Reaction with $HO^{\bullet}$ always plays a secondary role. The back-reduction processes increase the relative role of $HO^{\bullet}$, and the $HO^{\bullet}$

reaction becomes a very important if not the main pathway of aniline phototransformation. In the most extreme back-reduction scenario (Scenario 3, **Figure 5c**), the reaction with $HO^{\bullet}$ would prevail at low DOC and would play a comparable role as $^{3}CDOM^{*}$ at high DOC. The back-reduction processes also slow down significantly the photodegradation kinetics of aniline, with an important increase in the relevant lifetimes.

## 4. Conclusions

- Back-reduction by phenolic compounds is operational in the case of the $CO_3^{\bullet-}$-mediated photodegradation of anilines and sulfadiazine.
- The observed similarities concerning back-reduction for $CO_3^{\bullet-}$-induced and triplet-sensitized degradation suggest that the same reaction intermediates are involved in both cases.
- The operational conditions by which $CO_3^{\bullet-}$ is photogenerated (photolysis of nitrate or persulfate) affect the experimental values of $[AO]_{½}$ for aniline, presumably as a consequence of the different formation of additional reducing species in different systems.
- In sunlit surface waters scenarios, back-reduction decreases the contributions of both $CO_3^{\bullet-}$ and $^{3}CDOM^{*}$ to aniline photodegradation. In the absence of back-reduction, $HO^{\bullet}$ would always be a secondary process and aniline photodegradation would be dominated by $CO_3^{\bullet-}$ at low DOC and by $^{3}CDOM^{*}$ at high DOC. In contrast, $HO^{\bullet}$ and $^{3}CDOM^{*}$ play comparable roles at high DOC with back-reduction. Moreover, in the strongest back-reduction scenario for the $CO_3^{\bullet-}$ process, aniline photodegradation at low DOC would be dominated by $HO^{\bullet}$.

## References


Boreen, A.L., Arnold, W.A., McNeill, K., 2005. Triplet-Sensitized Photodegradation of Sulfa Drugs Containing Six-Membered Heterocyclic Groups: Identification of an SO2 Extrusion Photoproduct. Environ. Sci. Technol. 39, 3630–3638. https://doi.org/10.1021/es048331p

Boreen, A.L., Arnold, W.A., McNeill, K., 2003. Photodegradation of pharmaceuticals in the aquatic environment: A review. Aquat. Sci. 65, 320–341. https://doi.org/10.1007/s00027-003-0672-7

Bossmann, S.H., Oliveros, E., Göb, S., Siegwart, S., Dahlen, E.P., Payawan, L., Straub, M., Wörner, M., Braun, A.M., 1998. New Evidence against Hydroxyl Radicals as Reactive Intermediates in the Thermal and Photochemically Enhanced Fenton Reactions. J. Phys. Chem. A 102, 5542–5550. https://doi.org/10.1021/jp980129j

Buxton, G. V, Greenstock, C.L., Helman, P.W., Ross, A.B., 1988. Critical Review of rate constants for reactions of hydrated electrons, hydrogen atoms and hydroxyl radicals ($^{\bullet}OH/^{\bullet}O^{-}$) in Aqueous Solution. J. Phys. Chem. Ref. Data 17, 513–886. https://doi.org/https://doi.org/10.1063/1.555805

Canonica, S., Kohn, T., Mac, M., Real, F.J., Wirz, J., Von Gunten, U., 2005. Photosensitizer method to determine rate constants for the reaction of carbonate radical with organic compounds. Environ. Sci. Technol. 39, 9182–9188. https://doi.org/10.1021/es051236b

Canonica, S., Laubscher, H.U., 2008. Inhibitory effect of dissolved organic matter on triplet-induced oxidation of aquatic contaminants. Photochem. Photobiol. Sci. 7, 547–551. https://doi.org/10.1039/b719982a

Canonica, S., Schönenberger, U., 2019. Inhibitory Effect of Dissolved Organic Matter on the Transformation of Selected Anilines and Sulfonamide Antibiotics Induced by the Sulfate

Radical. Environ. Sci. Technol. 53, 11783–11791. https://doi.org/10.1021/acs.est.9b04105

Carena, L., Proto, M., Minella, M., Ghigo, G., Giovannoli, C., Brigante, M., Mailhot, G., Maurino, V., Minero, C., Vione, D., 2018. Evidence of an Important Role of Photochemistry in the Attenuation of the Secondary Contaminant 3,4-Dichloroaniline in Paddy Water. Environ. Sci. Technol. 52, 6334–6342. https://doi.org/10.1021/acs.est.8b00710

Carena, L., Puscasu, C.G., Comis, S., Sarakha, M., Vione, D., 2019. Environmental photodegradation of emerging contaminants: A re-examination of the importance of triplet-sensitised processes, based on the use of 4-carboxybenzophenone as proxy for the chromophoric dissolved organic matter. Chemosphere 237, 124476. https://doi.org/10.1016/j.chemosphere.2019.124476

Criquet, J., Leitner, N.K.V., 2009. Degradation of acetic acid with sulfate radical generated by persulfate ions photolysis. Chemosphere 77, 194–200. https://doi.org/https://doi.org/10.1016/j.chemosphere.2009.07.040

Dean, J.A., 1999. Lange's Handbook of Chemistry. 15th ed, 15th ed. ed. McGraw-Hill: New York, Etc.

Elango, T.P., Ramakrishnan, V., Vancheesan, S., Kuriacose, J.C., 1984. Reaction of the carbonate radical with substituted anilines. Proc. Indian Acad. Sci. - Chem. Sci. 93, 47–52. https://doi.org/10.1007/BF02841982

Erickson, P.R., Walpen, N., Guerard, J.J., Eustis, S.N., Arey, J.S., McNeill, K., 2015. Controlling Factors in the Rates of Oxidation of Anilines and Phenols by Triplet Methylene Blue in Aqueous Solution. J. Phys. Chem. A 119, 3233–3243. https://doi.org/10.1021/jp511408f

Galbavy, E.S., Ram, K., Anastasio, C., 2010. Chemistry 2-Nitrobenzaldehyde as a chemical

644 actinometer for solution and ice photochemistry. J. Photochem. Photobiol. A Chem. 209,
645 186–192. https://doi.org/10.1016/j.jphotochem.2009.11.013
646 Hao, Z., Ma, J., Miao, C., Song, Y., Lian, L., Yan, S., Song, W., 2020. Carbonate Radical
647 Oxidation of Cylindrospermopsin (Cyanotoxin): Kinetic Studies and Mechanistic
648 Consideration. Environ. Sci. Technol. 54, 10118–10127.
649 https://doi.org/10.1021/acs.est.0c03404
650 Herrmann, H., Reese, A., Zellner, R., 1995. Time-resolved UV/VIS diode array absorption
651 spectroscopy of SOx−(x=3, 4, 5) radical anions in aqueous solution. J. Mol. Struct. 348,
652 183–186. https://doi.org/https://doi.org/10.1016/0022-2860(95)08619-7
653 Huang, J., Mabury, S.A., 2000a. A New Method for Measuring Carbonate Radical Reactivity
654 toward Pesticides. Environ. Toxicol. Chem. 19, 1501–1507.
655 https://doi.org/https://doi.org/10.1002/etc.5620190605
656 Huang, J., Mabury, S.A., 2000b. Steady-state concentrations of carbonate radicals in field
657 waters. Environ. Toxicol. Chem. 19, 2181–2188.
658 https://doi.org/https://doi.org/10.1002/etc.5620190906
659 Huie, R.E., Clifton, C.L., 1990. Temperature dependence of the rate constants for reactions of
660 the sulfate radical, SO4-, with anions. J. Phys. Chem. 94, 8561–8567.
661 https://doi.org/10.1021/j100386a015
662 Jonsson, M., Lind, J., Eriksen, T.E., Merényi, G., 1994. Redox and Acidity Properties of 4-
663 Substituted Aniline Radical Cations in Water. J. Am. Chem. Soc. 116, 1423–1427.
664 https://doi.org/10.1021/ja00083a030
665 Liu, T., Yin, K., Liu, C., Luo, J., Crittenden, J., Zhang, W., Luo, S., He, Q., Deng, Y., Liu, H.,
666 Zhang, D., 2018. The role of reactive oxygen species and carbonate radical in
667 oxcarbazepine degradation via UV , UV/H2O2 : Kinetics , mechanisms and toxicity
668 evaluation. Water Res. 147, 204–213. https://doi.org/10.1016/j.watres.2018.10.007

669 Mack, J., Bolton, J.R., 1999. Photochemistry of nitrite and nitrate in aqueous solution: a
670 review. J. Photochem. Photobiol. A Chem. 128, 1–13.
671 https://doi.org/https://doi.org/10.1016/S1010-6030(99)00155-0
672 Millero, F.J., Pierrot, D., Lee, K., Wanninkhof, R., Feely, R., Sabine, C.L., Key, R.M.,
673 Takahashi, T., 2002. Dissociation constants for carbonic acid determined from field
674 measurements. Deep. Res. Part I Oceanogr. Res. Pap. 49, 1705–1723.
675 https://doi.org/https://doi.org/10.1016/S0967-0637(02)00093-6
676 Neta, P., Huie, R.E., Ross, A.B., 1988. Rate Constants for Reactions of Inorganic Radicals in
677 Aqueous Solution. J. Phys. Chem. Ref. Data 17, 1027.
678 https://doi.org/https://doi.org/10.1063/1.555808
679 NIST, 2004. Critically Selected Stability Constants of Metal Complexes Database. Stand. Ref.
680 Data Program, Vol.46. Natl. Inst. Stand. Technol. U.S. Dep. Commer.
681 Padmaja, S., Neta, P., Huie, R.E., 1993. Rate constants for some reactions of inorganic
682 radicals with inorganic ions. Temperature and solvent dependence. Int. J. Chem. Kinet.
683 25, 445–455. https://doi.org/https://doi.org/10.1002/kin.550250604
684 Remucal, C.K., 2014. The role of indirect photochemical degradation in the environmental
685 fate of pesticides: a review. Environ. Sci. Process. Impacts 16, 628–653.
686 https://doi.org/10.1039/c3em00549f
687 Ricci, M.C., Cross, R.F., 1993. Capillary electrophoresis separation of sulphonamides and
688 dihydrofolate reductase inhibitors. J. Microcolumn Sep. 5, 207–215.
689 https://doi.org/https://doi.org/10.1002/mcs.1220050305
690 Vialaton, D., Richard, C., 2002. Phototransformation of aromatic pollutants in solar light:
691 Photolysis versus photosensitized reactions under natural water conditions. Aquat. Sci.
692 64, 207–215. https://doi.org/10.1007/s00027-002-8068-7
693 Vione, D., 2020. A Critical View of the Application of the APEX Software (Aqueous

694 Photochemistry of Environmentally-Occurring Xenobiotics) to Predict Photoreaction
695 Kinetics in Surface Freshwaters. Molecules 25, 9.
696 https://doi.org/https://doi.org/10.3390/molecules25010009
697 Vione, D., Fabbri, D., Minella, M., Canonica, S., 2018. Effects of the antioxidant moieties of
698 dissolved organic matter on triplet-sensitized phototransformation processes:
699 Implications for the photochemical modeling of sulfadiazine. Water Res. 128, 38–48.
700 https://doi.org/10.1016/j.watres.2017.10.020
701 Vione, D., Minella, M., Maurino, V., Minero, C., 2014. Indirect Photochemistry in Sunlit
702 Surface Waters: Photoinduced Production of Reactive Transient Species. Chem. Eur. J.
703 20, 10590–10606. https://doi.org/10.1002/chem.201400413
704 Wegelin, M., Canonica, S., Mechsner, K., Fleischmann, T., Pesaro, F., Metzler, A., 1994.
705 Solar water disinfection: Scope of the process and analysis of radiation experiments.
706 Aqua J. Water Supply Res. Technol. 43, 154–169.
707 Wenk, J., Canonica, S., 2012. Phenolic antioxidants inhibit the triplet-induced transformation
708 of anilines and sulfonamide antibiotics in aqueous solution. Environ. Sci. Technol. 46,
709 5455–5462. https://doi.org/10.1021/es300485u
710 Wenk, J., Von Gunten, U., Canonica, S., 2011. Effect of Dissolved Organic Matter on the
711 Transformation of Contaminants Induced by Excited Triplet States and the Hydroxyl
712 Radical. Environ. Sci. Technol. 45, 1334–1340. https://doi.org/10.1021/es202028w
713 Willett, K.L., Hites, R.A., 2000. Chemical Actinometry : Using o-Nitrobenzaldehyde to
714 Measure Light Intensity in Photochemical Experiments. J. Chem. Educ. 77, 900–902.
715 https://doi.org/https://doi.org/10.1021/ed077p900
716 Wojnárovits, L., Tóth, T., Takács, E., 2020. Rate constants of carbonate radical anion
717 reactions with molecules of environmental interest in aqueous solution : A review. Sci.
718 Total Environ. 717, 137219. https://doi.org/10.1016/j.scitotenv.2020.137219

719 Yan, S., Liu, Y., Lian, L., Li, R., Ma, J., Zhou, H., Song, W., 2019. Photochemical formation
720 of carbonate radical and its reaction with dissolved organic matters. Water Res. 161,
721 288–296. https://doi.org/10.1016/j.watres.2019.06.002
722 Yan, S., Song, W., 2014. Photo-transformation of pharmaceutically active compounds in the
723 aqueous environment: a review. Environ. Sci. Process. Impacts 16, 697–720.
724 https://doi.org/10.1039/C3EM00502J